Electrochemical Study of $[Ni_6(\mu_3\text{-}Se)_2(\mu_4\text{-}Se)_3(dppf)_3]$ Cluster and Its Catalytic Activity towards the Electrochemical Reduction of Carbon Dioxide†

Deog-Su Park,‡ Md. Abdul Jabbar, Hyun Park,§ Hak Myoung Lee, Sung-Chul Shin,# and Yoon-Bo Shim*

*Department of Chemistry, Pusan National University, Busan 609-735, Korea. *E-mail: ybshim@pusan.ac.kr*
‡Center for Innovative BioPhysio Sensor Technology, Pusan National University, Busan 609-735, Korea
§Advanced Ship Engineering Research Center, Pusan National University, Busan 609-735, Korea
#Department of Chemistry, Gyeongsang National University, Chinju 660-701, Korea
Received June 5, 2007

The redox behavior of a $[Ni_6(\mu_3\text{-}Se)_2(\mu_4\text{-}Se)_3(Fe(\eta^5\text{-}C_5H_4P\text{-}Ph_2)_2)_3]$ (= [Ni-Se-dppf], dppf = 1,1-bis(diphenylphosphino)ferrocene) cluster was studied using platinum (Pt) and glassy carbon electrodes (GCE) in nonaqueous media. The cluster showed electrochemical activity at the potential range between +1.6 and −1.6 V. In the negative region (0 to −1.6 V), the cluster exhibited two-step reductions. The first step was one-electron reversible, while the second step was a five-electron quasi-reversible process. On the other hand, in the positive region (0 to +1.6 V), the first step involved one-electron quasi-reversible process. The applicability of the cluster was found towards the electrocatalytic reduction of CO_2 and was evaluated by experiments using rotating ring disc electrode (RRDE). RRDE experiments demonstrated that two electrons were involved in the electrocatalytic reduction of CO_2 to CO at the Se-Ni-dppf-modified electrode.

Key Words : Redox behavior of metal cluster, Surface modification, Electrocatalysis, Electrochemical reduction of CO_2

Introduction

Cluster electrochemistry is considered a promising field, due to their behavior as an electron reservoir,[1] allowing many reversible one-electron-transfer reactions to take place. Most clusters undergo multiple one-electron redox steps; several examples of multi-electron reaction involving structural changes have been reported in reviews on transition metal cluster electrochemistry.[2,3] Metal clusters have been widely used to elucidate structure and function of the biological systems.[4,5] In particular, a bidentate ligand, 1,1'-bis(diphenylphosphino) ferrocene (dppf = $Fe(\eta^5\text{-}C_5H_4Pph_2)_2$) has attracted continuous attention due to its interesting structure and has shown redox properties to its metal compounds.[6] It can also be utilized in the preparation of polymetallic complexes where the metal centers exhibit combinational effects such that the polymetallic complex behave differently from the sum of the individual moieties. In fact, molecules containing redox active-multimetallic centers are one of the hot topics in inorganic electrochemistry.[7] In particular, transition metal clusters containing redox active ferrocene ligands have attracted much attention in recent years,[8-11] because they often offer catalytic activities. Utilizing the dppf analogue of 1,3-bis(diphenylphosphino)indene, the preparation, isolation, and characterization of its selenium adduct and a heterometallic complex containing molybdenum and iron have been synthesized.[12] It has been observed, that the transition metal clusters containing redox active ligands show catalytic properties towards the electrochemical reduction of CO_2.[13-17] Increasing CO_2 concentration in the atmosphere is a major global concern and the reduction of CO_2 is a topic of considerable interest and extensively reviewed.[13,18] Electrocatalytic reduction of CO_2 mediated by transition metal complexes of terdentate ligands derived from diacetylpyridine[19] and water soluble Co- and Ni-phthalocyanines[20] have been reported. In addition, multinuclear iron-sulfur clusters were also found to catalyze the reduction of CO_2.[21]

In the present work, we report the electrochemical behaviour and redox mechanism of the [Ni-Se-dppf] metal cluster and catalytic electrochemical reduction of CO_2. Cyclic voltammetry (CV), controlled potential coulometry (CPC), and double potential step chronocoulometry (CC) were employed to investigate the redox behaviour of the cluster and its provable electrochemical redox mechanism. Electron spectroscopy for chemical analysis (ESCA) was used to characterize the cluster and RRDE was employed to analyze the mechanistic pathways and kinetic parameters for the electrochemical reduction of CO_2 at the cluster modified GCE surface.

Experimental

Chemicals. The [Ni-Se-dppf] cluster (shown in Figure 1) was synthesized according to the method described elsewhere.[22] Anhydrous methylene chloride, CH_2Cl_2 (Aldrich Co., Sure/Seal™) solvent was used as received and without further purification. Tetrabutylammonium perchlorate (TBAP, Fluaka, USA) was used as a supporting electrolyte, where it was recrystallized twice from ethanol followed by drying at 110 C in a vacuum oven at a reduced pressure for

†This paper is dedicated to professor Sang Chul Shim on the occasion of his honorable retirement.

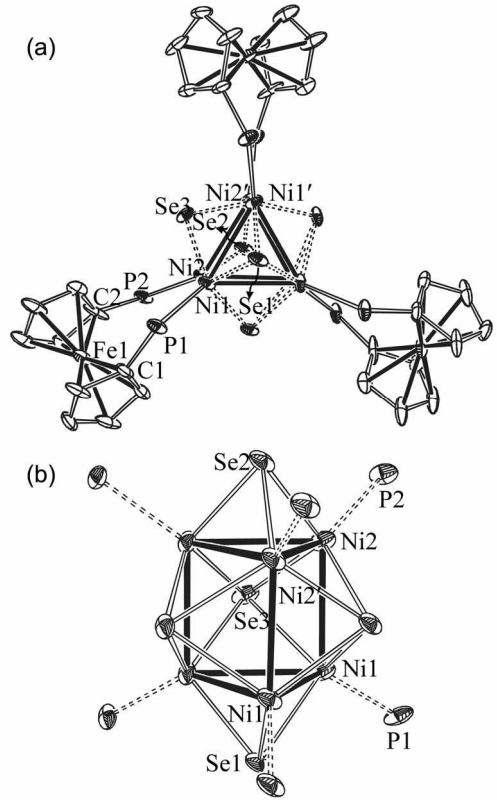

Figure 1. Structures of (a) the $[Ni_6(\mu_3\text{-}Se)_2(\mu_4\text{-}Se)_3(dppf)_3]$ cluster and (b) the core site.

over 24 hours before use.

Equipments. CV was performed using KOSENTECH KST-PI (Korea) and BAS-50 (Bioanalytical Systems, West Lafayette, IN, USA) electrochemical analyzers equipped with a conventional cell. Pt and GC electrodes (each 3 mm in diameter) were used as working electrodes and a Pt-wire as counter electrode. For the CPC experiment, Pt-mesh was used as working electrode and Pt-wire as counter electrode and they were separated from each other by a lug-in-capillary. For all the experiments, $Ag/AgNO_3$ in acetonitrile was used as the reference electrode. Before each experimental run, the Pt or GC electrodes were pretreated by polishing the surface with 0.3 and 0.05 μm α-alumina respectively.

The ESCA analysis was performed using a VG Scientific Escalab 250 XPS spectrometer using monochromated Al K_α source with charge compensation at the Korea Basic Science Institute (KBSI Busan Center). Rotating ring-disc electrode (RRDE) experiments were performed using a PINE Model AFRDE5 Bi-Potentiostat connected to a KOSENTECH-8 channel Data Acquisition System DA-1, a PC, and an EG&G (Princeton Applied Research) Model 636 Ring-Disk Electrode System.

Working solutions. The working solution for the voltammetric measurements was 0.1 mM of the metal cluster in a 0.1 M $TBAP/CH_2Cl_2$ solution. In case of CPC, 0.05 mM of the metal cluster was used and subjected to bulk electrolysis at a Pt-mesh electrode. Before each run, nitrogen gas was purged through the solution for twenty minutes and a continuous stream of nitrogen gas-flow was maintained above the surface of the working solution. All voltammetric measurements were performed at room temperature and pressure.

[Ni-Se-dppf] modified GCE electrode preparations for CO_2 reduction. For the preparation of the [Ni-Se-dppf] modified GCE, 20 μL of 0.1 mM [Ni-Se-dppf] cluster dissolved in a CH_2Cl_2 solvent was carefully transferred to the clean GCE surface and the solvent was allowed to evaporate at room temperature. The modified electrode was kept at 60 ×C for at least four hours to remove the rest of the organic solvent from the electrode surface before use. For the RRDE experiment, the glassy carbon disk (area 0.459 cm^2) was modified by the metal cluster in a similar way above, whereas the glassy carbon ring electrode remained unmodified.

Results and Discussion

Cyclic voltammetric behavior. Figure 2 shows the CV recorded for the cluster, containing a 0.1 M $TBAP/CH_2Cl_2$ solution. The sweep toward the negative region (0 to −1.6 V) revealed two reduction processes (peak I at −0.46 V and peak II at −1.46 V in Figure 2). The associated oxidation peaks in the reverse scan was observed at −1.38 V (peak II' in Figure 1) and −0.39 V (peak I' in Figure 2), respectively. On the other hand, multi-oxidation processes were observed in the positive potential region (0 to +1.6 V). The oxidation process was observed at 0.6 V (peak III' in Figure 2); the

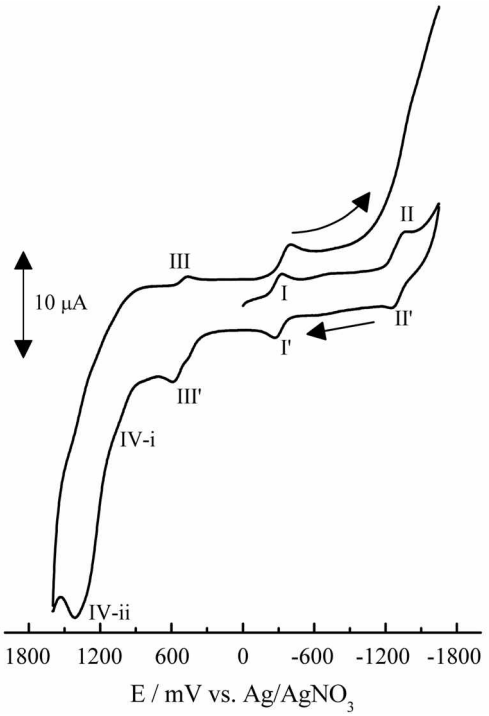

Figure 2. The CV recorded for the Ni-Se-dppf cluster in a 0.1 M $TBAP/CH_2Cl_2$ solution at a glassy carbon electrode. Scan rate: 100 mV/s.

Table 1. Data from the cyclic voltammetric recorded for 0.1 mM $[Ni_6(\mu_3\text{-}Se)_2(\mu_4\text{-}Se)_3(dppf)_3]$ in a 0.1 M TBAP/CH_2Cl_2 solution at a platinum electrode with different scan rates

Scan rate /mVs^{-1}	Step I		Step II		Step III	
	ΔE_p/mV	i_{pa}/i_{pc}	ΔE_p/mV	i_{pa}/i_{pc}	ΔE_p/mV	i_{pa}/i_{pc}
50	55	1.05	64	0.74	70	2.34
75	55	1.06	69	0.84	70	2.36
100	58	1.10	75	0.85	71	2.40
125	62	1.12	75	0.88	71	2.93
150	62	1.15	79	0.88	74	3.35
175	64	1.16	79	0.89	74	3.72
200	66	1.16	80	0.89	76	3.78

other oxidation peaks were observed at +1.06 V (peak IV-i in Figure 2) and +1.40 V (peak IV-ii in Figure 2), respectively. The associated reduction peak of IV-i and IV-ii were absent in the CV, whereas a reduction peak was slightly split corresponding to the anodic peak III' in Figure 2. Numerical data from the CV for the cluster were summarized in Table 1. By studying the relevant electrochemical data tabulated in Table 1, it was found that the I/I' peaks were reversible and the II/II', III' peaks were quasi-reversible, respectively. On the other hand, the processes occurring at the IV-i and IV-ii peaks were irreversible.

Controlled potential coulometry (CPC). CPC of 0.05 mM of the metal cluster in a 0.1 M TBAP/CH_2Cl_2 solution at a Pt-mesh electrode was performed to elucidate the number of electrons involved in each step and hence derive the electron-transfer mechanism. The numbers of electrons involved in each of the electrochemical process was calculated as one by using the following equation,

$$n = \frac{Q}{FN} \tag{1}$$

where, n = no. of electrons participating in the individual process; Q = total amount of charge consumed by the individual processes; N = no. of moles of the substrate = m/M; where 'm' is the amount of the substrate taken, and 'M' is the molar mass of the substrate. The net charge (background subtracted), evaluated for the process involving the redox peaks of I/I' (−0.45/−0.39 V) was 0.0495 C, which indicated a one electron process. Similarly, the second peaks at −1.46/−1.38 V(peaks II/II') consumed a net charge of 0.268 C, indicating the involvement of five electrons. The oxidation peak at +0.6 V (peak III') required 0.041 C for the one-electron oxidation process, whereas, for the oxidation peaks at +1.06 V and +1.40 V (peak IV-i and IV-ii), 0.387 C in total were required for the eight-electron oxidation process. In this process, the color of the cluster solution was changed from dark brown to colorless indicating that the structural change of the cluster might have taken place or it decomposed over +1.2 V.

Double potential step chronocoulometry (CC). CC of a 0.1 mM of the metal cluster solution was performed to elucidate the number of electrons involved in each step, to see whether the adsorption phenomenon takes place in the

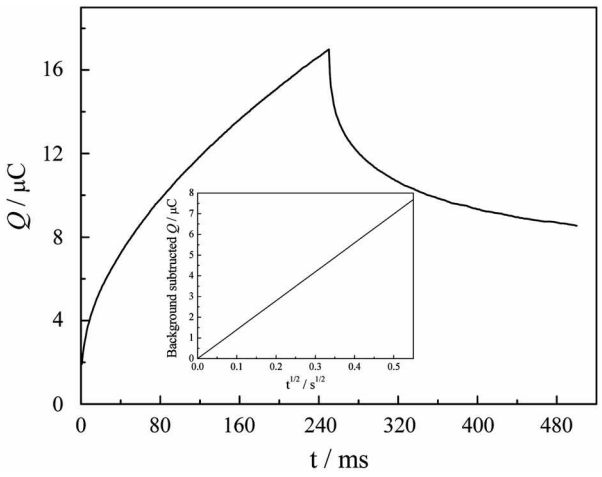

Figure 3. The chronocoulometric response of 0.1 mM $[Ni_6(\mu_3\text{-}Se)_2(\mu_4\text{-}Se)_3(dppf)_3]$ in a 0.1 M TBAP/CH_2Cl_2 solution at a platinum electrode for step I. Inset figure: background-subtracted charge *vs.* square root of time for the forward step.

corresponding processes. The potential windows of the CC experiments for the peaks I/I' and II/II' were −0.25/−0.60 V and −1.15/−1.50 V, respectively. On the other hand, the potential windows of the peak III' and IV-i/IV-ii were +0.25/+0.75 V and +1.0/+1.50 V, respectively. The pulse width was set at 250 msec for all the steps. Figure 3 shows the chronocoulometric response at the Pt disk electrode for peaks I/I'. The number of electrons involved in individual processes and the charge in the redox processes were calculated by using the following equation[23]:

$$Q = \frac{2nFAD_o^{1/2}C_o t^{1/2}}{\pi^{1/2}} + Q_{dl} + nFA\Gamma_o \tag{2}$$

where, Q_{dl}, is the capacitative charge and Γ_o is the amount of adsorbed species (mol cm^{-2}). The Q–$t^{1/2}$ plot of equation (2) will give a straight line with a slope of $2nFAD_o^{1/2}C_o/\pi^{1/2}$ and intercept, $Q_{dl} + nFA\Gamma_o$, from which 'n' can be calculated from the slope and Γ_o of the adsorbed species can easily be calculated from the intercept of the background subtracted Q–$t^{1/2}$ plot. The diffusion coefficients 'D' for the individual steps were evaluated from CV data.

Individual peak assignments of the [Ni-Se-dppf] metal cluster. In order to assign redox processes, CVs were recorded for ferrocene, dppf, and [Ni-Se-dppf] cluster in a CH_2Cl_2/0.1 M TBAP solution and represented in Figure 4(a), (b) and (c), respectively. The two pairs of peaks at the negative potential region (0 to −1.6 V) were assigned as the electron transfer processes occurring in the $[Ni_6Se_5]$-cluster core. Among them, the first redox peak was one-electron reversible and the second one was five-electron quasi-reversible. The results of CC experiments suggested that there was no adsorption on the electrode surface for these two processes at GCE. These results can be compared to the previously obtained data for the cluster $[Ni_3Se_2(dppe)_3][BPh_4]$[24] in which two chemically reversible couples were found in the negative potential region in DMF solution.

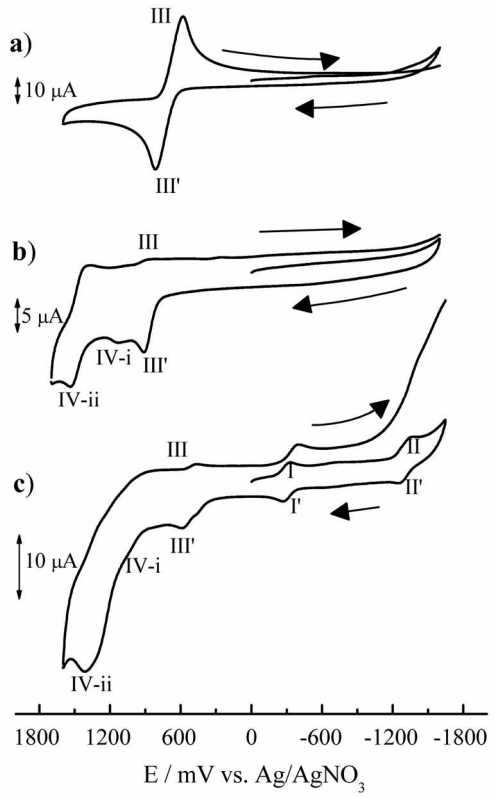

Figure 4. CVs recorded for a) ferrocene b) dppf, c) Ni-Se-dppf cluster in a 0.1 M TBAP/CH_2Cl_2 solution at a glass carbon electrode. Scan rate: 100 mV/s.

However, the peak positions were not coinciding with the [Ni-Se-dppf] clusters because of the difference between the ligands dppe and dppf and their electronically connective abilities towards the metals. By comparing CVs between [Ni-Se-dppe] and [Ni-Se-dppf] clusters, it was clear that the electron transfer process was easier in [Ni-Se-dppf] than [Ni-Se-dppe] cluster, because [Ni-Se-dppf] cluster possessed lower reduction potential.

On the other hand, the redox processes in the positive potential region (0 to +1.6 V) were confirmed by comparing the CVs between ferrocene (Figure 4a), the ligand dppf (Figure 4b), and metal cluster (Figure 4c). The oxidation peak of ferrocene, which was observed at +0.8 V (Figure 4a) was shifted towards a more positive potential region, *i.e.* +0.9 V (peak III' in Figure 4b), in the dppf ligand. However, the ferrocene-centered peak was shifted towards a more negative potential of +0.56 V (peak III' in Figure 4c) in the case of [Ni-Se-dppf] cluster. The shifting of this peak towards the negative potential direction can be due to the electron-donating property of the metal cluster, which makes it easier for the oxidation of ferrocene. The CC data suggested that the adsorption reaction took part in this region. Two oxidation peaks at +1.06 V (peak IV-i in Figure 4c) and +1.40 V (peak IV-ii in Figure 4c) in the metal cluster were assigned by comparing the dppf ligand, where the similar oxidation peaks were observed at +1.13 (peak IV-i in Figure 4b) and +1.54 V (peak IV-ii in Figure 4b). These two oxidation peaks are due to the oxidation of the phosphine groups in the dppf ligand as mentioned above. It is to be noted that only the oxidation peak corresponding to the redox reaction of dppf ligand was observed below the scan rate of 100 mV/s. On the other hand, the reduction peak corresponding to the anodic peak at +0.9 V appeared apparently above 100 mV/s. By increasing the scan rate to over 100 mV/s, the I_{pa}/I_{pc} ratio gradually reaches the value of unity. This means that the reaction should follow an EC mechanism. The chronocoulometric data at the GCE showed that the adsorption reaction had taken place during the oxidation of ferrocene moiety. Thus, pairs of small peaks at +1.13 and +1.54 V might be associated with the adsorption peaks of dppf molecules. The adsorption process was confirmed with chronocoulometry at GCE and the amount of adsorbed dppf was calculated to be 2.1×10^{-10} mol/cm^2. The cathodic peaks appearing at +0.85 and +1.4 V were assigned as the reduction peaks of phosphine group. This was confirmed by performing a separate cyclic voltammogram recorded for triphenylphosphine (not shown in the figure). It showed an irreversible anodic peak at +0.86 V. However, redox process of the phosphine group in the dppf molecular was more electrochemically reversible due to the formation of stable bonds between the phosphine groups and the ferrocene moieties. Accordingly, in [Ni-Se-dppf] cluster, a single-electron irreversible process was due to the ferrocene moiety following chemical complication at +0.56 V (peak III' in Figure 4c) and the eight-electron irreversible process was due to the oxidation of diphosphine in the dppf moiety (peak IV-i and IV-ii in Figure 4c). It was observed that the homologous cluster [$Ru_3(\mu$-Se)$_2$(dppf)(CO)$_7$] would undergo either multi-electron irreversible reduction or oxidation in which dppf first exhibits a ferrocene-centered one-electron oxidation, accompanied by slow chemical complications and a further irreversible two-electron oxidation centered on the two phosphine subunits in the metal cluster.[25] This suggested a single dppf moiety required three electrons in total for the oxidation process.

Proposed redox mechanism of [Ni-Se-dppf] cluster. Studying the redox behavior with CV, CPC, CC, and RRDE experiments made assigning peaks at each step for the [Ni-

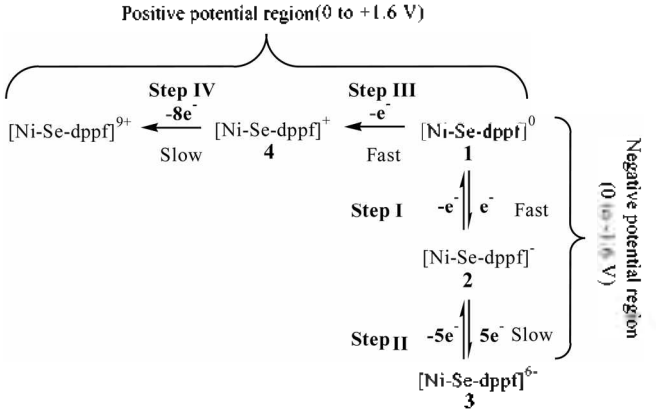

Scheme 1. Proposed redox mechanism for the electrochemical reaction of the [Ni-Se-dppf] cluster.

Se-dppf] cluster and the following tentative redox mechanism (Scheme 1) was proposed. According to Scheme 1, cluster '1' was first reduced reversibly to give '2' involving a one-electron process. In the step II, it was further reduced to produce the species '3' involving a five-electron process at the negative potential region. On the other hand, at the positive potential region of step III, the cluster '1' showed a ferrocene-centered one-electron irreversible oxidation to yield the species '4'. In CPC, there was no change in color of the cluster solution during the above processes, suggesting that the cluster undergoes electron-transfer without any structural change at this potential range. On the other hand, the cluster solution turned from dark brown to colorless during the eight-electron oxidation process suggesting that the cluster had decomposed and structural change had occurred in the step IV. In total, nine electrons (peak III', IV-i, and IV-ii in Figure 1) involved in the decomposition process can easily be attributed to the individual ferrocene and diphenylphosphene moieties. Among them, three electrons were involved in the oxidation of three ferrocene units, and six-electrons were involved in the oxidation of three diphenylphosphine subunits as discussed in the previous section.

Catalytic Current from the Electrochemical Reduction of CO_2 at a [Ni-Se-dppf] Modified GCE

Cyclic voltammetric study. The applicability of the cluster was found towards the generation of catalytic current during the electrochemical reduction of CO_2. The generation of catalytic currents from the electrochemical reduction of CO_2 in aqueous solution was observed at a [Ni-Se-dppf] metal cluster modified GCE. For this purpose, a clean GCE was modified by [Ni-Se-dppf] cluster in a CH_2Cl_2 solution. In order to examine the catalytic current for the electrochemical reduction of CO_2 at the [Ni-Se-dppf] metal cluster modified GCE, separate CVs at a bare GCE and a metal-cluster modified GCE in N_2 and CO_2 atmosphere were carried out in the aqueous 0.1 M KCl solution and represented in Figure 5. A small reduction peak at −1.38 V was observed at a bare GCE in a 0.1 M KCl solution saturated with CO_2, whereas a large reduction peak (I_{pc} = 300 μA) was observed at the cluster modified GCE in the same solution. The reduction peak potential was shifted towards the positive potential direction to about 0.28 V and was observed at −1.10 V. The extra current and the shifting of potential arose due to the catalytic property of the metal cluster towards the electroreduction of CO_2. Therefore, the metal cluster modified GCE can reduce CO_2 and also lower the reduction potential which is far away from the hydrogen overpotential.

ESCA analysis of the cluster modified GCE surface. The cluster modified GCE surface was further examined by ESCA before and after CO_2 reduction. This suggested that the oxidation state of nickel was changed during the electrochemical reduction of CO_2, whereas selenium remained unchanged during the process. It was also found that, nickel existed as Ni(II) on the GCE surface before the electro-

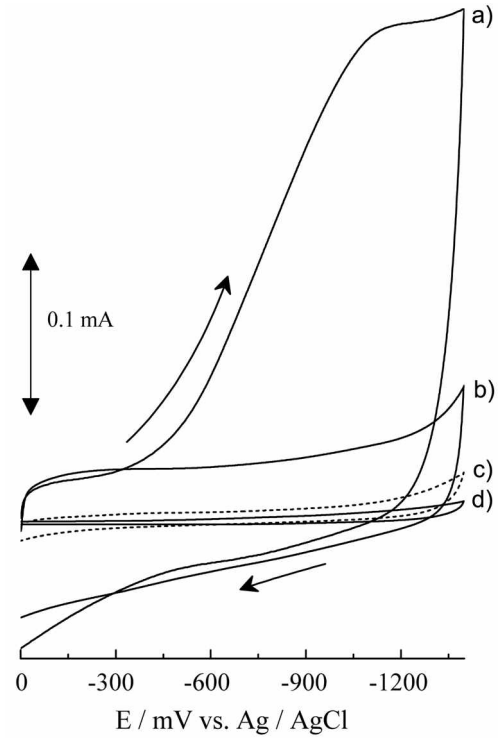

Figure 5. CVs recorded for a Ni-Se-dppf modified electrode in a 0.1 M KCl solution under a) CO_2 and b) N_2 atmospheres. c) & d) are CVs for a bare GCE in CO_2 and N_2 atmospheres. The scan rate: 100 mV/s.

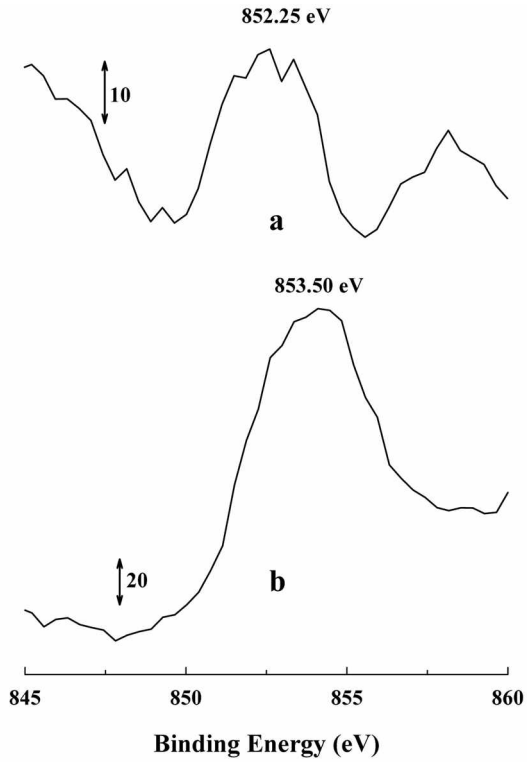

Figure 6. ESCA spectra of [Ni-Se-dppf] modified GCE a) before and b) after CO_2 reduction.

chemical reduction of CO_2. After the electrochemical reduction of CO_2, a mixture of Ni(I)/Ni(II) (95%/5%) was detected on the GCE surface. This suggested that Ni was first existed as Ni(II) before reaching the potential of −0.3 V during electrochemical treatment; it was further reduced to Ni(I) during the electrochemical reduction of CO_2 because of a sufficient negative potential. The ESCA of the cluster was represented in Figure 6 before and after electrochemical reduction of CO_2.

RRDE studies on CO_2 reduction. Typical ring disk voltammetry results obtained for the electrochemical reduction of CO_2 at the cluster modified GC disk and bare GC ring electrode at different rotation speeds are shown in Figure 7a. The disk I-E curve is similar to the stationary state voltmmogram which was shown in Figure 5. At the ring electrode, the wave current increased with increasing rotation rate. This signified that the product produced at the cluster modified disk of the RRDE was detected by the ring electrode. The 'n'-value was calculated using least square analysis of the I-E plot of the disk electrode and applying the Levich equation (Equation 3). It was found that two electrons were involved in the electrochemical reduction of CO_2 at the cluster modified GC-disk electrode.

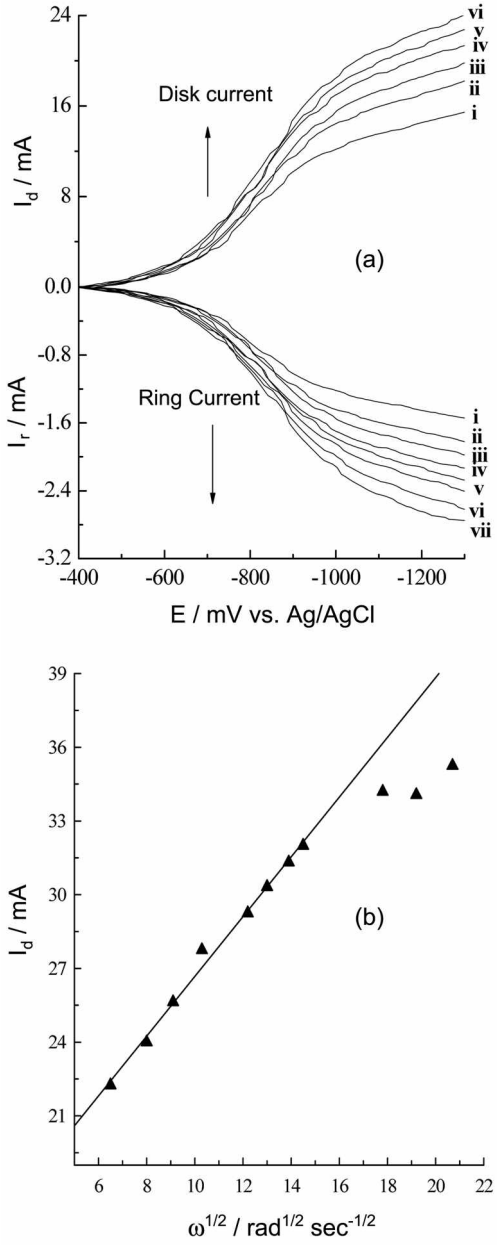

Figure 7. (a) The hydrodynamic voltammograms recorded for a [NiSe-dppf] modified-GC disc (upper part); and GC ring (lower part), during the electrochemical reduction of CO_2 in a 0.1 M KCl solution at different rotation speeds (from lower to upper, ω: 41.90, 83.81, 167.62, 209.52, 314.29, 366.67, 419.05 rad/sec). Ring potential: −1.2 V. (b) The I_d *vs.* $\omega^{1/2}$ plot obtained for the disk electrode.

$$I_D = 0.6205\, nFA_d D^{2/3} \upsilon^{-1/6} \omega^{1/2} C_{CO_2} \quad (3)$$

Here, A_d: 0.459 cm^2; $D^{2/3} = (1.91 \times 10^{-5})^{2/3}$ [26]: 7.10×10^{-4} cm^2/sec; $\upsilon^{-1/6} = 2.17$ cm^2/sec and $C_{CO_2} = 1.022 \times 10^{-2}$ M. The least square analysis data for the I-E curve (Figure 7b) is as follows: From the I_d *vs.* $\omega^{1/2}$ plot with the Levich equation (least square parameters: Y = A + B * X; where A: 14.5195; B: 1.2156, R: 0.9928). Over the higher rotation speed than 315 rad/s, the plot was curved due to the slow electrochemical kinetics.

It has been reported widely that one of the main products of CO_2 reduction catalyzed by metal complexes is CO.[27,28] The transition metal complex (CoPc) deposited on the carbon electrode promote the reduction of CO_2 to CO via the equation (4) at −0.65 V ($E^{0'}(CO_2/CO)$).[28]

$$CO_2 + 2e^- + 2H^+ \rightarrow CO + H_2O \quad (4)$$

The ring current at an applied potential of −1.2 V as shown in Figure 7(a) was corresponded to the reduction of CO and was confirmed by cyclic voltammetry using authentic CO gas. In order to examine the reduction of CO at a bare GCE, CVs were recorded under N_2 and CO atmospheres in a 0.1 M KCl solution. The CO reduction peak on a bare glassy carbon electrode in the CO saturated solution appeared at −0.6 V (*vs.* Ag/AgCl). The reduction current increased due to the concentration change of authentic CO gas. Thus, it can be predicted that CO was preferably formed from the electrochemical reduction of CO_2. The electrochemical reduction of CO at a Cu electrode in various electrolyte solutions was examined.[29] The reaction products from the Cu electrode were CH_4, C_2H_4, C_2H_5OH, CH_3OH, CH_3CHO, and C_2H_5CHO.

RRDE experimental results also demonstrated that two electrons were involved in the electrocatalytic reduction of CO_2 at the Se-Ni-dppf-modified electrode. Therefore, the reduction of CO_2 on the cluster modified disc electrode can be assigned as in equation (4).

The percentage yield of CO formation (Φ) was calculated using the following relation[30] comparing the disk and ring current at constant rotation rate:

$$\phi = \frac{200 I_R / N_o}{I_D + I_R / N_o} \quad (5)$$

At the rotation rate of 1400 rev/min, and w of 104.7619 rad/s, I_R and I_D was recorded as 1.77 and 11.66 mA respectively

and hence Φ was calculated which was close to 99%. The collection efficiency (N_o) was calculated from a separate experiment and obtained as 0.152.

Conclusion

We studied for the redox behavior of a [Ni-Se-dppf] cluster and proposed its redox mechanism from the results of cyclic voltammetry, controlled potential coulometry, and double potential step chronocoulometry. The multiple electron transfer steps were observed as follows: In the negative potential region in the CVs, the cluster exhibited two-step redox processes. The first step was one-electron reversible, while the second step was five-electron quasi-reversible processes. On the other hand, in the positive potential region, the first step involved one-electron quasi-reversible process and the second, third steps shows partial degradation of the cluster over +0.8 V. We confirmed the application of the cluster towards the electrocatalytic reduction of CO_2 to CO with a cluster modified GCE. The RRDE experiment suggested that CO_2 reduction produced CO and the reduction involved two electrons, which was confirmed with the authentic CO gas.

Acknowledgement. This work was supported by Pusan National University Research Grant (2004) and SRC program of KOSEF (R11-2000-070-07001).

References

1. Lauher, J. W. *J. Am. Chem. Soc.* **1978**, *100*, 5305; **1979**, *101*, 2604.
2. Lemoine, P. *Coord. Chem. Rev.* **1982**, *47*, 56.
3. Lemoine, P. *Coord. Chem. Rev.* **1988**, *83*, 169.
4. Burrows, C. J.; Muller, J. G. *Chem. Rev.* **1998**, *98*, 1109.
5. Erkkila, K. E.; Odom, D. T.; Barton, J. K. *Chem. Rev.* **1999**, *99*, 2777.
6. Gan, K.-S.; Hor, T. S. A. *Ferrocenes* Togni, A.; Hayashi, T., Eds.; VCH: New York, 1995; pp 3-104.
7. Kaim, W.; Klein, A.; Glockle, M. *Acc. Chem. Res.* **2000**, *33*, 755 and references therein.
8. Wong, W.-Y.; Wong, W. T. *J. Chem. Soc. Dalton Trans.* **1996**, 3209.
9. Lau, C. S.-W.; Wong, W.-T. *J. Organomet. Chem.* **1999**, *588*, 113.
10. Adams, R. D.; Qu, B. *Organometallics* **2000**, *19*, 2411.
11. Adams, R. D.; Qu, B. *Organometallics* **2000**, *19*, 4090.
12. Adams, J.; Berry, D. E.; Browing, J.; Burth, D.; Curnow, O. J. *J. Organomet. Chem.* **1999**, *580*, 245.
13. Arakawa, H.; Aresta, M.; Armor, J. N.; Barteau, M. A.; Beckman, E. J.; Bell, A. T.; Bercaw, J. E.; Creutz, C.; Dixon, D. A.; Domen, K.; DuBois, D. L.; Eckert, J.; Fijita, E.; Gibson, D. H.; Goddard, W. A.; Goodman, D. W.; Keller, J.; Kubas, G. J.; Kung, J. E.; Lyons, L. E.; Manzer, T. J.; Marks, K.; Morokuma, K. M. Nicholas, R.; Periana, H. H.; Que, L.; Rosteup-Nielson, J.; Sachtler, W. M. H.; Schmidt, L. D.; Sen, A.; Somorajai, G. A.; Stair, P. C.; Stults, B. R.; Tumas, W. *Chem Rev.* **2001**, *101*, 953.
14. Fujita, E.; Brunschwig, B. S. *Homogeneous Redox Catalysis of CO_2 Fixation*; Balzani, V., Ed.; Wiley-VCH: Weinheim, 2001; Vol. IV, pp 88-126.
15. Darensbourg, D. J.; Rokicki, A. *J. Am. Chem. Soc.* **1982**, *104*, 349.
16. Darensbourg, D. J. *The Organometallic Chemistry of Carbon Dioxide Pertinent to Catalysis*; Branden, C. I.; Schneider, G., Eds.; Oxford University Press: 1994; p 111.
17. Kim, S. G.; Kim, D. H.; Kang, D. M.; Jabbar, Md. A.; Min, G. S.; Shim, Y.-B.; Shin, S. C. *Bull. Korean Chem. Soc.* **2005**, *26*, 1603.
18. Taniguchi, I. *Modern Aspect of Electrochemistry*; Bockris, J.O'M.; White, R. E.; Conway, B. E., Eds.; Plenum Press: New York, 1989; Vol. 20, Chapter 5.
19. Chiericato Jr., G.; Arana, C. R.; Casado, C.; Caudrado, I.; Abruna, H. D. *Inorg. Chem. Acta* **2000**, *300*, 32.
20. Alwis, C. D.; Crayston, J. A.; Cromie, T.; Eisenblatter, T.; Hay, R. W.; Lampeka, Y. D.; Tsymbal, L. V. *Electrochim. Acta* **2000**, *45*, 2061.
21. Tezuka, M.; Yajima, T.; Tsuchiya, A.; Matsumoto, Y.; Uchida, Y.; Hidai, M. *J. Am. Chem. Soc.* **1982**, *104*, 6834.
22. Kang, D. M.; Shin, S. C. Preparation and synthesis of the cluster, submitted.
23. Bard, A. J.; Faulkner, L. R. *Electrochemical Methods, Fundamentals and Applications*; Wiley: New York, 2001; pp 210-243.
24. Matsumoto, K.; Ikuzawa, M.; Kamikubo, M.; Ooi, S. *Inorg. Chem. Acta* **1994**, *217*, 129.
25. de Biani, F. F.; Graiff, C.; Opromolla, G.; Predieri, G.; Tiripicchio, A.; Zanello, P. *J. Organomet. Chem.* **2001**, *637*, 586.
26. *CRC Hanbook of Chemistry and Physics*; Lide, D. R., Ed.; CRC press LLC: 2000; pp 6-191.
27. Lieber, C. M.; Lewis, N. S. *J. Am. Chem. Soc.* **1984**, *106*, 5033.
28. Zagal, J. H. *Coord. Chem. Rev.* **1992**, *119*, 85.
29. Yoshio, H.; Ryutaro, T.; Yuzuru, Y.; Akira, M. *J. Phy. Chem. B* **1997**, *101*, 7075.
30. Bron, M.; Bogdanoff, P.; Fiechter, S.; Dorbandt, I.; Hilgendorff, M.; Schulenburg, H.; Tributsch, H. *J. Electranal. Chem.* **2001**, *500*, 510.